SF2A 2007
J. Bouvier, A. Chalabaev, C. Charbonnel (eds)

X-RAY AFTERGLOW LIGHT CURVES : TOWARD STANDARD CANDLE ?

B. Gendre[1], A. Galli[1] and M. Boër[2]

Abstract. We investigate the clustering of afterglow light curves observed in X-ray and in optical before the launch of SWIFT in light of SWIFT observations. We have constructed a sample of 34 bursts with known distance and X-ray afterglow. This sample includes bursts observed by BeppoSAX, XMM-Newton, Chandra, and SWIFT. We correct the light curves for cosmological effects and compare the observed X-ray fluxes at 1 day after the burst. We check if there is any correlation between the observed flux and the burst spectral and temporal properties. We find that X-ray afterglow light curves cluster in luminosity, even in the SWIFT era. We show that this clustering is due only to the afterglow, and that the inclusion of prompt-related data broaden the distribution and hide the clustering. The same clustering is observed in optical, and we found three sub-division between optical and X-ray *bright* afterglows, *dim* ones, and optically *bright* -X-ray *dim* ones. We argue that the observed optical and X-ray clustering are related to the fireball total energy, the external medium density, the fraction of fireball energy going in relativistic electrons and magnetic fields. These parameters are either all fixed to a standard value, or all linked together.

1 Introduction

Long Gamma-Ray Bursts (GRBs) are linked with the death of massive stars (for a review, see Meszaros 2006). Their association with supernovae (e.g. Hjorth et al. 2003, Stanek et al. 2003) and the fact that these events are at cosmological distance (Metzger 1997) make them interesting for studies of cosmology and hint for a high distance standard candle. However, while the GRB features a prompt emission, usually seen in gamma-ray only, and an afterglow seen at all wavelengths, only the former emission has been considered for cosmological studies yet.

The afterglow emission is less studied from a cosmological point of view because of its diversity. However, there were hints of standardization of the X-ray afterglows. The first attempt was done by Boër & Gendre (2000), who found a hint of clustering in the X-ray light curves of BeppoSAX afterglows. This clustering was confirmed by Gendre & Boër (2005) when adding the XMM-Newton and Chandra afterglow observations. We will refer to these articles as paper I and II. In addition, Kouveliotou et al. (2004) showed that supernova and GRB light curves had similar behaviors and were converging with time toward a similar luminosity. In paper I, we tried also to check if optical light curves were also presenting a clustering but failed due to the poor knowledge of the host intrinsic absorption at that time. This study was completed by Nardini et al. (2006) and Liang & Zhang (2006) who found independently that optical afterglows were also clustering in luminosity.

The revolution of the SWIFT era, which provide a large sample of X-ray observations with a redshift estimation, allowed us to increase our sample of events. With this larger sample, we have tried to derive a method for estimating the burst redshift from the X-ray light curve (Gendre & Boër 2006). However, this still needs to understand the nature of these two groups and a way to derive the group belonging of each burst. This is the purpose of this article. In Section 2 we present our sample and the data analysis. We discuss the X-ray clustering in Section 3. We compare the X-ray and optical clusterings in Section 4, before concluding.

[1] IASF-Roma, via fosso del cavaliere 100, 00133, Roma, Italy
[2] Observatoire de Haute Provence, 04870, Saint Michel L'observatoire, France

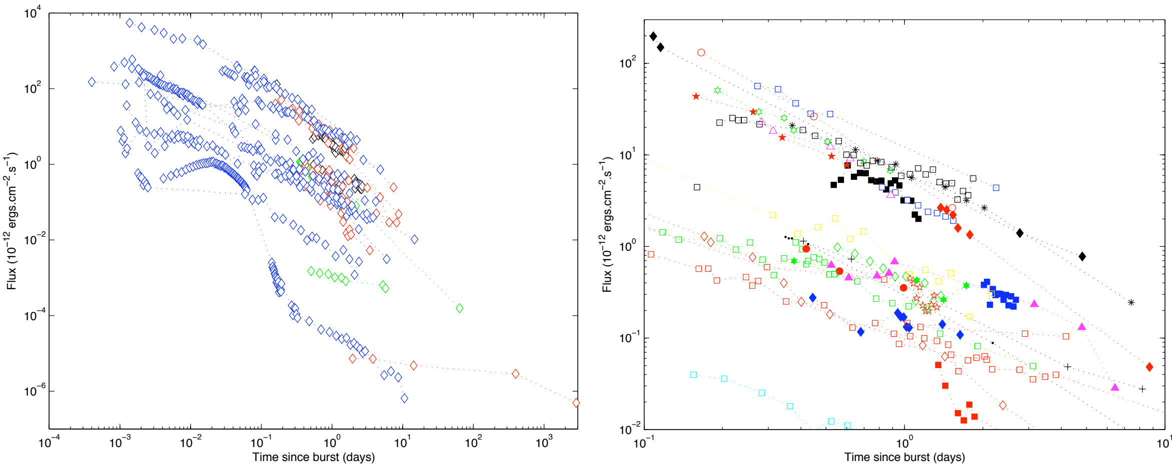

Fig. 1. The corrected light curves of our sample. Left panel: full scale to show all bursts. We indicate SWIFT, XMM-Newton, Chandra and BeppoSAX bursts with blue, green, black and red diamonds respectively. Right panel: we display the same light curves restricted to the time interval from 0.1 to 10 days after the GRB. Each burst is displayed using a different symbol/color combination. In both panels the error bars are not displayed for clarity.

2 X-ray afterglow sample and analysis

Our sample is listed in Gendre et al. (2007b). It is composed by GRBs with known redshift and X-ray afterglow observations. This include all afterglows observed by BeppoSAX, XMM-Newton and Chandra, which data were retrieved from De Pasquale et al. (2006) and Gendre et al. (2006). As for SWIFT observations, we included several bursts, taken from the XRF catalog of Gendre et al. (2007a) or randomly selected from archive. We removed the flaring parts of the light curve when applicable. We corrected these flux light curves for distance effects as in Paper I and II : applying a k-correction using the measured spectral index of each afterglow, using a flat universe with $\Omega_m = 0.3$, and correcting the time dilation effect by computing the luminosity at a time t using the observed flux at time $t \times (1 + z)$. We restricted the light curves to the 2.0−10.0 keV X-ray band, where the absorption is negligible. This allowed us to neglect any other corrections for absorption by the ISM. We do not take into account any beaming due to a possible jet.

Instead of using a luminosity light curve, we express all light curves in flux units at a given distance (like the optical absolute magnitude). This is again to reduce the uncertainties on the correction. For consistency with paper I and II, we fix it to $z = 1$.

3 Results

Figure 1 presents the corrected light curves. As one can clearly see in the left part of the figure, no clustering is observed in the early part of the light curves. In fact, the addition of SWIFT bursts seems to have blurred out the clustering observed in paper I and II. However, a more careful inspection of the figure (right panel) still indicates a clustering, but only in the late part of the afterglow emission.

SWIFT has shown that the X-ray light curve is composed by a first steep power-law segment, associated with the tail of prompt emission, followed by a flat plateau, a second steepening, and a possible late steepening related to the jet aperture (Nousek et al. 2006). Willingale et al. (2007) have interpreted this behavior with a two-components model. According to them, the plateau phase marks the transition between a first component (the prompt) and a second one (the afterglow). We have retrieved for SWIFT bursts the values of T_a, which correspond to the end of the plateau phase, and excluded all SWIFT data taken before this time. Results are displayed in Fig. 2.

The two groups reported in papers I and II are now clearly seen. We refer to the bright group as *group I* and the dimmer one as *group II*, as in paper II. They are clustering with a mean flux of 6.2×10^{-12} erg s^{-1} cm^{-2} and 3.1×10^{-13} erg s^{-1} cm^{-2} for groups *I* and *II* respectively. We also see some bursts not clustering : GRB 980425, GRB 031203, GRB 060218, and GRB 060512. These ones are all nearby events, with the more

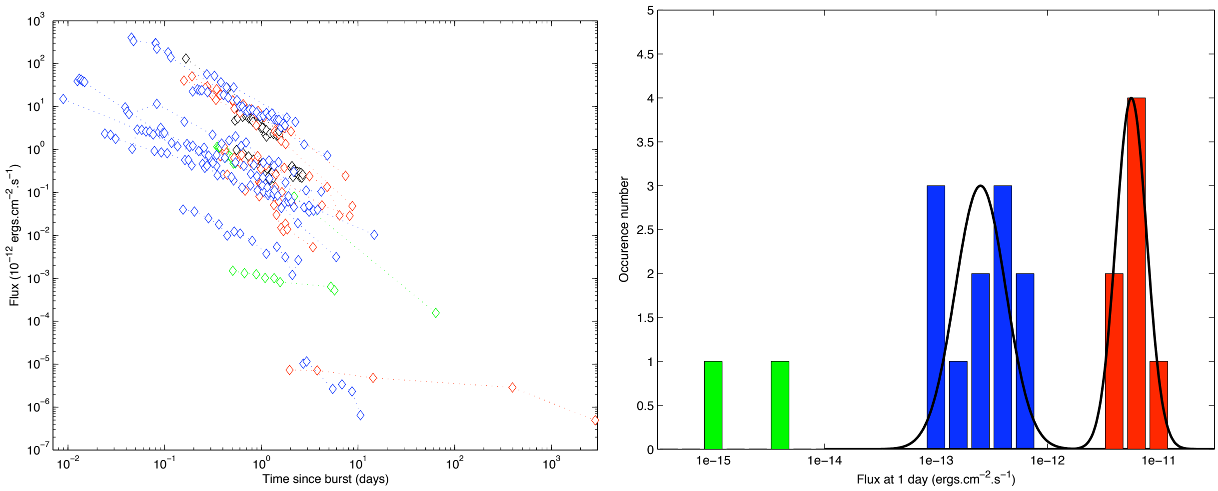

Fig. 2. Left : the corrected light curves of our sample, using only data taken after the plateau phase for SWIFT bursts. Colors are the same than in Fig. 1. The two groups indicated in papers I and II are now clearly seen. Right : a distribution of fluxes observed at one day after the burst. The solid lines are the best fit Gaussian distribution of the groups fluxes. In the following figures, red refers to bright events, blue to intermediate luminosity events and green to under-luminous events. See electronic version for colors.

distant of them, GRB 060512, being at $z = 0.4428$ (Bloom et al. 2006). Note however that GRB 030329 is also at low redshift, but clusters in *group II*, so that the low redshift deviation is not a rule for all bursts. We prefer to call all these low luminosity events *group III* bursts.

The probability that a power law luminosity distribution (letting the index be a free parameter) represent the observed distribution is, at the maximum, 3.56×10^{-8}, thus the observed clustering in two groups is very significant. To compute this probability we impose a lower luminosity limit such that the *group III* bursts are excluded, because of the selection effects (see Sec. 4).

We checked if this clustering was due to the isotropic burst energy E_{iso} or the peak energy E_p values. The two groups share a similar E_p distribution. This also holds for the E_{iso} distribution.

In paper II, we pointed out a possible segregation of decay indexes : *group I* bursts seemed to decay faster than *group II* ones. Thanks to SWIFT and its fast monitoring, we can clearly rule out this hypothesis : no obvious difference can be seen in the decay index distributions of the two groups. The situation is similar when looking at the spectral indexes : the two distributions are similar.

4 Discussion

4.1 Distance effects and bias

Figure 3 presents the redshift distribution of our sample. One can clearly see a trend : low luminosity bursts are nearby while bright ones are more distant. This is even more obvious if one include the *group III* bursts, which have all a very low redshift. This effect can be partly explained by a selection effect, as low luminosity events cannot be detected at high distance. The lack of dim distant events (located in the upper left corner of Fig. 3) is due to that effect. However, we should also detect bright nearby events. Our nearest *group I* burst (GRB 991216) is located at $z = 1.02$. While this is already lower than the mean SWIFT GRB redshift (2.7, Jakobsson et al. 2006), one may wonder why we do not observe a bright *group I* event with $z \sim 0.5$, and we still have to understand if this is related to the nature of *group I* bursts.

4.2 The optical afterglows

Nardini et al. (2006) and Liang & Zhang (2006) have discovered that even in optical, afterglow light curves are clustering. They do not include in their work any of our *group III* bursts, so we will restrict the following discussion only to groups *I* and *II*. They found two groups, and we will refer to them as *optical group I* (or *oI*)

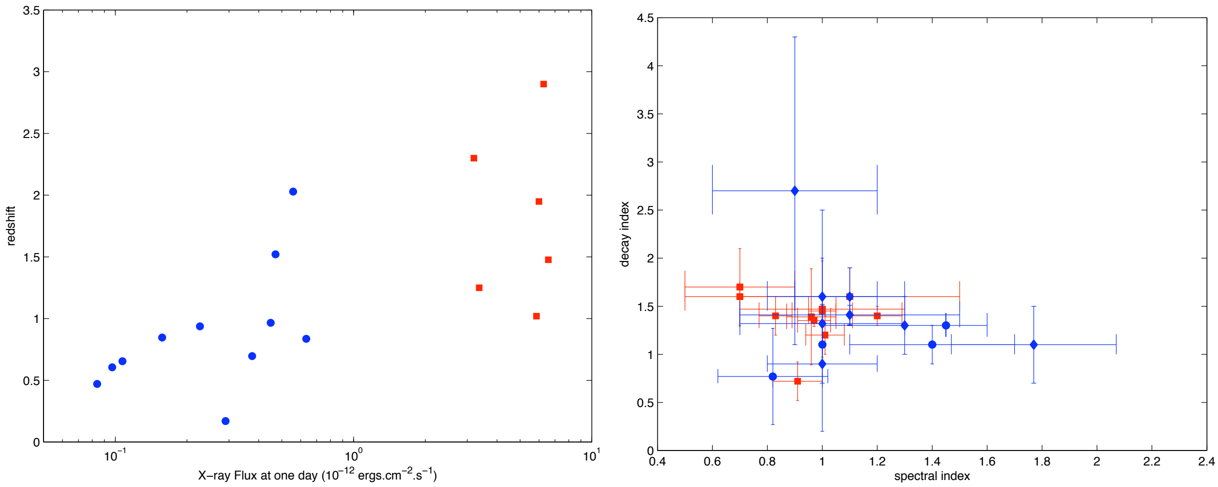

Fig. 3. Left : distribution of the redshifts of the groups *I* and *II*. Right : decay index versus spectral index. We indicate on that figure bursts bright both in X-ray and optical (red squares), bursts dim both X-ray and optical (blue circles), and bursts bright in optical and dim in X-ray (blue diamonds).

and *optical group II* (or *oII*) for the bright and dim group respectively. According to Liang & Zhang (2006), one day after the burst (rest frame), the difference in luminosity between groups *oI* and *oII* is ~ 26. At the same time, the difference in luminosity between the X-ray groups is ~ 24.

We found that, while an *optical group I* burst can belong to *group I* or *group II* in X-ray, *optical group II* bursts are all dim in X-ray. We present in Fig. 3 the repartition in the decay index versus spectral index space of those three kinds of bursts. Again, no clear separation can be observed between these different kind of events.

4.3 The fireball model

We have used the fireball model predictions to investigate further on the nature of the observed clusterings. Nardini et al. (2006) has indicated that for almost all bursts, we have $\nu_m < \nu_{optical} < \nu_c < \nu_X$. We will assume this repartition. According to Panaitescu & Kumar (2000), during the slow cooling regime the predicted flux for a fireball expanding in a uniform InterStellar Medium (ISM) is:

$$\begin{aligned} F_\nu &= 10^{2.1+0.7p} D_{28}^{-2} \nu_{14.6}^{-(p-1)/2} t_d^{-3(p-1)/4} \\ &\quad \times E_{B,\,53}^{(p+1)/4} E_{e,\,53}^{p-1} E_{53}^{2-p} (n_*/E_{53})^{1/2} mJy \\ &\qquad (\nu_m < \nu < \nu_c) \end{aligned} \tag{4.1}$$

$$\begin{aligned} F_\nu &= 10^{0.4+0.7p} D_{28}^{-2} \nu_{14.6}^{-p/2} t_d^{-(3p-2)/4} \\ &\quad \times E_{B,\,53}^{(p-2)/4} E_{e,\,53}^{p-1} E_{53}^{2-p} mJy \\ &\qquad (\nu_c < \nu) \end{aligned} \tag{4.2}$$

while for a fireball expanding in a wind-like medium we have:

$$\begin{aligned} F_\nu &= 10^{2.3+0.8p} D_{28}^{-2} \nu_{14.6}^{-(p-1)/2} t_d^{-(3p-1)/4} \\ &\quad \times E_{B,\,53}^{(p+1)/4} E_{e,\,53}^{p-1} E_{53}^{2-p} (A_*/E_{53}) mJy \\ &\qquad (\nu_m < \nu < \nu_c) \end{aligned} \tag{4.3}$$

$$\begin{aligned} F_\nu &= 1.35 \times \left(\tfrac{17}{72}\right)^{p/4} \times 10^{0.4+0.7p} D_{28}^{-2} \nu_{14.6}^{-p/2} t_d^{-(3p-2)/4} \\ &\quad \times E_{B,\,53}^{(p-2)/4} E_{e,\,53}^{p-1} E_{53}^{2-p} mJy \\ &\qquad (\nu_c < \nu) \end{aligned} \tag{4.4}$$

where p is the usual electron distribution power law index (we assume $p = 2.1$ for all bursts), and $E_B = \epsilon_B E$, $E_e = \epsilon_e E$ the energy carried by the magnetic field and electrons respectively (E is the fireball total energy). D, ν, and t are the distance, observation frequency and observation time respectively.

X-ray group	Optical group	Medium class	E_e constraint	E_B constraint	E constraint
I	*oI*	ISM	$E_{e,53}^{1.2} = 0.0784 E_{53}^{1/6} n_0^{1/30}$	$E_{B,53} = 1.02 \times 10^{-4}(E_{53}/n_0)^{2/3}$	$0.0851 < E_{53}$
I	*oI*	wind	$E_{e,53}^{1.2} = 0.1449 E_{53}^{2/15} A_*^{1/15}$	$E_{B,53} = 0.91 \times 10^{-5}(E_{53}/A_*)^{4/3}$	$0.1635 < E_{53}$
II	*oI*	ISM	$E_{e,53}^{1.2} = 0.0032 E_{53}^{1/6} n_0^{1/30}$	$E_{B,53} = 5.51 \times 10^{-3}(E_{53}/n_0)^{2/3}$	$0.0039 < E_{53}$
II	*oI*	wind	$E_{e,53}^{1.2} = 0.0059 E_{53}^{2/15} A_*^{1/15}$	$E_{B,53} = 4.95 \times 10^{-4}(E_{53}/A_*)^{4/3}$	$0.0081 < E_{53}$
II	*oII*	ISM	$E_{e,53}^{1.2} = 0.0039 E_{53}^{1/6} n_0^{1/30}$	$E_{B,53} = 1.18 \times 10^{-4}(E_{53}/n_0)^{2/3}$	$0.0047 < E_{53}$
II	*oII*	wind	$E_{e,53}^{1.2} = 0.0072 E_{53}^{2/15} A_*^{1/15}$	$E_{B,53} = 1.07 \times 10^{-5}(E_{53}/A_*)^{4/3}$	$0.0098 < E_{53}$

Table 1. Constraints on E_B, E_e, E, and the density parameter implied by the clustering observed in X-ray and in optical.

We extracted from the work of Nardini et al. (2006) the optical fluxes at 4.69×10^{14} Hz. They are 0.178 mJy and 10.0μJy for groups *oI* and *oII* respectively. The X-ray fluxes (at 4.8×10^{17} Hz) are 1.86 μJy and 0.09 μJy for groups *I* and *II* respectively.

Combining equation 4.2 with equation 4.1, and equation 4.4 with equation 4.3, we obtain the results listed in Table 1. One can note that the constraints on E_e are weakly density dependent (due to the very low exponent of the density parameter). Because $E_e < E$ (or $\epsilon_e < 1$), we can find a constraint on the total fireball energy E (a similar condition is true for E_B, but this is not constraining for E).

4.3.1 The fireball parameters

Within each group there are few variations of fluxes around the mean value. This may indicate that either E_B, E_e, E, and n_* (or A_*, depending on the surrounding medium) are all linked together, or are all fixed to a common value, with few variations allowed. In the former case, because the surrounding medium density is fixed *before* the burst occurs, it is this quantity that should be considered as the true variable parameter (and not the energy injected within the fireball).

If E_B, E_e, E, and A_* (or n_*) are all constant, the constraints on the model are strong because a GRB will occur inside a typical environment (3 kinds according to the 3 observed behaviors). If so, one can understand why we cannot observe a relativistic outflow associated with each type Ib/c supernovae (Soderberg et al. 2004) : in fact, those normal type Ib/c supernovae are then all *failed GRBs*.

4.3.2 The nature of the clustering

The flux ratio between the two optical groups and the two X-ray groups are similar. Panaitescu & Kumar (2002) have investigated the surrounding medium around 10 GRBs. They found that most of them can be fit with an ISM (all belonging to our optical and X-ray bright burst group), while only one burst needs a wind environment (it is an optical and X-ray dim burst). This could suggest that *group II-oII* bursts are surrounded by a stellar wind while *group I-oI* are located within an ISM. Assuming that the only difference between these two groups is due to the medium density profile (and thus that all other parameters have a similar distribution within the two groups), we can explain the difference between the two groups if we set $n_* = 6.09 A_*$. However in such a case we then cannot explain the behavior of *group II-oI* bursts. We also note that Panaitescu & Kumar (2002) have found that a wind medium can also accurately describe the surrounding environment of two *group I-oI* bursts. Thus, the surrounding medium class could not be the origin of the observed clustering.

In X-ray, the flux is mostly dependent on E_e and E (see eqn. 4.2 and 4.4). If one assumes that E_{iso} is a good estimator of E, then because of the observed similar distributions of E_{iso} of the two groups, different values of E cannot explain the differences between the two groups. This in turn would imply that it is E_e that varies within the two groups (see Table 1). This however again cannot explain the origin of *group II-oI*, because if the clustering is due only to a difference of E_e then we cannot expect from eqn. 4.1 and 4.2, and 4.3 and 4.4, a dim X-ray afterglow to be bright in optical. The constraints listed in Table 1 indicate that the difference between groups *I-oI* and *II-oII* on one hand, and group *II-oI* on the other hand can be also due to a different value of E_B.

We thus propose that the presence of different groups is ascribed to different families of E_e and E_B values:

- a family of 'magnetized fireball' that produces the group *II-oI*. In such a case the fireball transfers only a low fraction of its energy into relativistic electrons.
- a family of 'less magnetized fireball' that produces the groups *I-oI* and *II-oII*. The fraction of total energy going into magnetic fields is roughly one order of magnitude lower than group *II-oI*. These two groups can be related to an high and low fraction of energy going in relativistic electrons, respectively.

Interestingly, the group *II-oII* is not very numerous (compared to the other two groups), so that most of GRBs of our sample are then either 'magnetized but not electron-energized' or 'not magnetized but electron-energized'.

5 Conclusions

We have investigated the clustering of afterglow light curves observed in X-ray and in optical just by BeppoSAX, XMM-Newton and Chandra, in light of the well-monitored SWIFT light curves. Adding SWIFT bursts to the previous sample reported in paper II, we still observe the X-ray clustering. We adopted the formalism of Willingale et al. (2007) and found that it is the second component that clusters in luminosity. In fact we have shown that the clustering is not related to the properties of the prompt emission. A similar clustering was observed also in optical. We compared the classification within each group in X-ray and in optical, and found three sub-division: *bright* optical and X-ray afterglows, *dim* ones, and optically *bright*-X-ray *dim* ones. We proposed that this clustering is due to the fireball parameters and the surrounding medium density, which are either all constant or all linked together. This allowed us to put constraints on the values of ϵ_B and ϵ_E, and expressed them in terms of the total fireball energy and the surrounding medium density. We stress that the extension of this work at low frequency (radio, sub-millimeter and infrared) may help solving the exact origin of the clustering by strongly constraining the medium density and the position of the synchrotron self absorption and injection frequencies.

BG acknowledge support from COFIN grant 2005025417. We are please to thank Alessandra Corsi and Giulia Stratta for very useful and constructive discussions.

References

Bloom, J. S., Foley, R. J., Koceveki, D., & Perley, D., 2006, GCN #5217
Boër, M. & Gendre, B. 2000, A&A, 361, L21
Boër, M., Atteia, J.L., Damerdji, Y., et al., 2006, ApJ, 638, L71
Gendre, B., Boër, M., 2005, A&A , 430, 465
Gendre, B., Corsi, A., & Piro, L., 2005, A&A, 455, 803
Gendre, B., & Boër, M., 2006 AIPC, 836, 558
Gendre, B., Galli, A., Corsi, A., et al., 2007a, A&A, 462, 565
Gendre, B., Galli, A., Boër, M., submitted to ApJ, 2007b
Hjorth, J., Sollerman, J., Møller, P., et al. 2003, Nature, 423, 847
Jakobsson, P., Levan, A., Fynbo, J. P. U., et al., 2006, A&A, 447, 897
Kouveliotou, C., Woosley, S.E., Patel, A., et al., 2004, ApJ, 608, 872
Liang, E. & Zhang, B., 2006, ApJ, 638, L67
Metzger, M.R., Djorgovski, S.G., Kulkarni, S.R., et al., 1997, Nature, 387, 879
Meszaros, P, 2006, Rep. Prog. Phys., 69, 2259
Nardini, M., Ghisellini, G., Ghirlanda, G., et al., 2006, A&A, 451, 821
Nousek, J. A., Kouveliotou, C., Grupe, D., et al., 2006, ApJ, 642, 389
Panaitescu, A., & Kumar, P., 2000, ApJ, 543, 66
Panaitescu, A., & Kumar, P., ApJ, 571, 779, 2002
De Pasquale, M., Piro, L., Gendre, B., et al., 2005, A&A, 455, 813
Soderberg, A.M., Frail, D.A., & Wieringa, M.H., 2004, ApJ, 607, L13
Stanek, K. Z., Matheson, T., Garnavich, P. M., et al., 2003, ApJ, 591, L17
Watson, D., Reeves, J.N., Hjorth, J., et al., 2006, ApJ, 637, L69
Willingale, R., O'Brien, P. T., Osborne, J. P., et al., 2007, submitted to ApJ, astro-ph/0612031